Available online at www.sciencedirect.com
SCIENCE DIRECT®
Journal of Catalysis 220 (2003) 104–114
JOURNAL OF CATALYSIS
www.elsevier.com/locate/jcat

Direct decomposition of NO into N_2 and O_2 over La(Ba)Mn(In)O_3 perovskite oxide

Tatsumi Ishihara,[a,*] Makoto Ando,[a] Kenji Sada,[a] Keiko Takiishi,[a] Keiji Yamada,[b] Hiroyasu Nishiguchi,[a] and Yusaku Takita [a]

[a] *Department of Applied Chemistry, Faculty of Engineering, Oita University, Dannoharu 700, Oita 870-1192, Japan*
[b] *Graduate School of Engineering, Oita University, Dannoharu 700, Oita 870-1192, Japan*

Received 11 February 2003; revised 4 June 2003; accepted 4 June 2003

Abstract

Although $LaMnO_3$ perovskite oxide has been reported to exhibit low activity in NO direct decomposition into N_2 and O_2, doping Ga or In at the Mn site of La(Ba)MnO_3 has been found effective of increasing the activity for NO direct decomposition into N_2 and O_2. The activity of NO decomposition increased in the order Ba > Sr > Ca for the La site dopant, and In > Ga for the Mn site. Among the investigated dopants and compositions, the highest N_2 yield was achieved with $La_{0.7}Ba_{0.3}Mn_{0.8}In_{0.2}O_3$. On this catalyst, NO conversion increased with increasing reaction temperature, and at 1123 K, NO conversion into N_2 and O_2 attained values of 75 and 41%, respectively. The high yield of N_2 and O_2 was maintained for 12 h. Coexistence of oxygen decreased the N_2 yield with $P_{O_2}^{-0.53}$; however, a N_2 yield of 15% could be sustained even at 10% coexisting O_2 at 1073 K. The NO decomposition rate increased with increasing NO partial pressure and obeyed with $P_{NO}^{1.31}$. O_2 temperature-programmed desorption measurements showed that oxygen desorption was greatly enhanced by In doping at the Mn site. NO TPD also showed that the amount of NO adsorbed greatly increased with In doping. Therefore, improved activity of NO decomposition with In substitution seems to be caused by the weakening adsorption of oxygen and the increased adsorption of NO. IR measurements of adsorbed NO also suggest that the major adsorption species at high temperature was NO_3^- and it seems likely that NO decomposition proceeds after removal of NO_3^- and/or oxygen. N_2O direct decomposition on $La_{0.7}Ba_{0.3}Mn_{0.8}In_{0.2}O_3$ was further studied. It was found that $La_{0.7}Ba_{0.3}Mn_{0.8}In_{0.2}O_3$ is highly active in the direct decomposition of N_2O even under the coexistence of O_2. Therefore, decomposition of NO on $La_{0.7}Ba_{0.3}Mn_{0.8}In_{0.2}O_3$ may proceed via N_2O as the intermediate species.

Keywords: Nitrogen oxide; Direct decomposition; Perovskite oxide; $LaMnO_3$; N_2O decomposition; Dopant effects

1. Introduction

Nitrogen oxides (NO_x), which are mainly formed in an internal combustion engine, are extremely toxic to the human body and also harmful to the environment as a main source of acid rain. At present, several methods have been proposed for NO_x removal [1–3]. Among them, selective reduction of NO_x by hydrocarbons has been studied extensively, and various catalysts, in particular Cu-ZSM-5, have been reported as active catalysts for this reaction [4]. On the other hand, direct decomposition of NO into N_2 and O_2 ($2NO = N_2 + O_2$) is the most ideal reaction for NO_x removal because the process is quite simple. However, it is well known that the oxygen formed adsorbs strongly on the catalyst, resulting in deactivation of the catalyst. Some catalysts, such as Cu-ZSM-5 [5], Co-ZSM-5 (which contains Co in the framework [6]), La_2O_3 [7], Ba/MgO [8], and $LaCoO_3$ [9] based perovskite oxides, are active in the direct decomposition of NO. In particular, Teraoka et al. reported that $La_{0.8}Sr_{0.2}CoO_3$ is highly active in NO decomposition, and NO conversions into N_2 and O_2 reached values of 72 and 40%, respectively, at 1073 K [10]. Although the reaction temperature is high, high activity of NO decomposition is expected on perovskite oxides. In addition, the temperature of the exhaust gas at the engines outlet is higher than 1073 K. Increasing the reaction temperature is expected to decrease the negative effects of water and sulfur compounds.

In the present study, NO decomposition over $LaMnO_3$ perovskite oxide doped with Ga or In at the Mn site was

* Corresponding author.
E-mail address: ishihara@cstf.kyushu-u.ac.jp (T. Ishihara).

0021-9517/$ – see front matter
doi:10.1016/S0021-9517(03)00265-3

investigated. The activity of $LaMnO_3$-based oxide in NO decomposition is low, except for the doped $SrMnO_3$ mixed oxide of $Sr_{0.6}La_{0.4}Mn_{0.8}Ni_{0.2}O_3$ [10,11]. However, increasing the mobility of oxide ions in $LaMnO_3$ by doping with Ga or In may increase the activity of NO decomposition. This is because the doped $LaGaO_3$ perovskite oxide exhibits a high oxide ion mobility [12] and the rate-limiting step of this reaction on perovskite catalysts is considered the adsorption of NO into the coupled oxygen vacancy sites [10], and increasing the mobility of oxygen vacant by dopant seems to be a useful method for formation of the coupled oxygen vacancy sites. A relationship between NO decomposition and oxide ion conductivity is also predicted on a brownmillerite oxide [13].

2. Experimental

2.1. Preparation of catalyst

Doped $LaMnO_3$ was prepared by a conventional solid-state reaction method. The precursor of $LaMnO_3$ was obtained by evaporating the aqueous solution of a calculated amount of $La(NO_3)_3$, $Sr(NO_3)_2$, $Mn(CH_3COO)_2$, and metal nitrate acid. The mixtures obtained were calcined in air at 1273 K for 3 h. The sample obtained was measured with X-ray diffraction using a commercial diffract meter (Rigaku Rint-2500) with a Cu-K_α line. The catalyst powder thus obtained was pressed into disks, crushed, and sieved into 16 to 32 meshes.

2.2. NO, N_2O, and NO_2 decomposition reactions

Direct decomposition of NO, NO_2, and N_2O was performed with a conventional fixed-bed gas-flow reactor with a 12-mm-diameter quartz glass tube. Gaseous mixtures of 1% NO, 1% NO_2, or 10% N_2O diluted with He were fed to the catalyst bed for NO, NO_2, and N_2O direct decomposition reactions, respectively. One gram of the catalyst without dilution was always set in the reactor by using quartz wool (ca. 0.5 mm in catalyst height) and the feed rate of the reactant was fixed at $W/F = 3.0$ g s/cm^3, where W and F are the catalyst weight and the gas flow rate. Produced N_2, O_2, and the fed NO were analyzed with online gas chromatography with a molecular sieve 5A column and N_2O with a Polapac-Q column with a thermal conductivity detector (TCD). Because NO_2 cannot be analyzed with gas chromatography, an observed deficit in oxygen in the products may be connected to NO_2 formation in a cool zone after the reaction. Therefore, in this study, the activity of the catalyst in NO decomposition is discussed in terms of the N_2 yield. It is also noted that the formation of N_2O was not observed in this study.

The effects of the coexistence of O_2 were measured by mixing 10% O_2 diluted with He with the reactant gas. Concentrations of oxygen as well as NO or N_2O were controlled by changing the feed rate of He as a balance gas to keep the total flow rate of reactant at 20 ml/min constant.

2.3. Characterization of the catalyst

Temperature-programmed desorption of O_2 and NO was measured with a mass spectrometer (Anelva AQA-100R) as a detector. Standart TPD equipment consisting of a gas adsorption reactor connected to a mass spectrometer and an adsorption gas circulating line was used. Catalyst (0.3 g) was always fixed in the quartz tube (6 mm in diameter) with quartz wool. The catalyst was evacuated at 873 K for 1 h, exposed to oxygen or NO gas at 13.32 kPa for 0.5 h, and then cooled to room temperature in the sample gas atmosphere. After evacuation at room temperature for 0.5 h, desorption of the adsorbed oxygen or NO was measured at a heating rate of 10 K/min. The adsorption state of NO was also measured with an IR spectrometer (JASCO-610) with an MCT detector. Measurement was performed with the diffusion reflection unit using a KBr window and connecting to a gas-circulating and vacuum system. After evacuation at 873 K for 3 h, background spectra of the catalyst without NO adsorption were measured at each temperature. The catalyst was exposed to NO gas at 13.32 kPa and heated for 1 h in a gas-circulating system at the measurement temperature, and the IR measurement was performed at an elevated temperature.

3. Results and discussion

3.1. Effects of dopant on NO decomposition activity of $LaMnO_3$

Table 1 summarizes the activities of the examined catalysts doped with Ga at the B site of perovskite oxide (ABO_3) in NO decomposition at 15 min after the reaction started. Because NO conversion on the several catalysts examined, gradually decreased, NO decomposition activity at 15 min after reaction start is listed in Table 1. Although the reaction temperature was as high as 1073 K, all examined catalysts doped with Ga exhibited activity in NO direct decomposition, except the $LaCrO_3$ catalyst. No N_2O formation was observed on any catalyst examined. It is considered that the temperature range for activity is too high to form N_2O. The activity of NO decomposition decreased in the order $LaMnO_3 > LaCoO_3 > LaCuO_3 > LaFeO_3 \gg LaCrO_3$, which is almost the same tendency as that reported earlier [14]. It is clear that the yield of N_2 is always much higher than that of O_2. Therefore, an observed deficit of oxygen in the products may be connected with NO_2 formation in a cool zone after the reaction. However, even considering the formation of NO_2, the amount of oxygen formation was deficient on many catalysts. On these catalysts, such as $LaCuO_3$- or $LaFeO_3$-based oxides, the oxygen formed strongly adsorbs on the catalyst and the activity of NO decomposition

Table 1
NO direct decomposition into N_2 and O_2 over $LaMO_3$ (M = Cr,Fe,Cu,Co,Mn) catalyst

Catalyst	BET surface area (m^2/g)	Conversion (%)				
		Of NO	Into N_2	Into O_2	Into N_2O	Into NO_2[a]
$La_{0.7}Ba_{0.3}Cr_{0.8}Ga_{0.2}O_3$	1.9	3.8	4.1	0.1	0.0	0.0
$La_{0.7}Ba_{0.3}Fe_{0.8}Ga_{0.2}O_3$	3.1	48.9	31.3	1.5	0.0	17.6
$La_{0.7}Ba_{0.3}Cu_{0.8}Ga_{0.2}O_3$	1.0	58.4	40.7	3.9	0.0	17.7
$La_{0.7}Ba_{0.3}Co_{0.8}Ga_{0.2}O_3$	0.9	78.6	54.1	8.9	0.0	24.5
$La_{0.7}Ba_{0.3}Mn_{0.8}Ga_{0.2}O_3$	7.5	92.3	60.2	22.8	0.0	32.1
$La_{0.7}Sr_{0.3}Mn_{0.8}In_{0.2}O_3$	4.2	37.5	21.8	1.3	0.0	15.7
$La_{0.7}Ca_{0.3}Mn_{0.8}In_{0.2}O_3$	0.8	24.4	12.8	0.5	0.0	12.6
$La_{0.7}Ba_{0.3}Mn_{0.8}In_{0.2}O_3$	8.0	96.8	63.7	24.4	0.0	33.1
$La_{0.7}Ba_{0.3}Mn_{0.8}Al_{0.2}O_3$	7.0	89.7	59.7	14.5	0.0	30.0
In_2O_3	4.5	4.2	1.8	0.0	0.0	2.4

[a] Estimated based on material balance of nitrogen. Catalyst, 1 g; 1.0% NO in He; $W/F = 3.0\ \mathrm{g\,s\,cm^{-3}}$. Temperature, 1073 K.

may be decreased by the adsorbed oxygen after a longer period. In Table 1, the BET surface area is also summarized. However, it is apparent that no clear relationship between surface area and NO decomposition activity was observed. Among the examined perovskite catalysts doped with Ga, $LaMnO_3$-based oxide exhibited a fairly high N_2 yield, and the formation of O_2 was also observed. Therefore, in the following, NO direct decomposition on doped $LaMnO_3$ was studied in detail. Because $LaMnO_3$-based oxide exhibits the largest BET surface area in the Ba-doped catalyst, the large surface area might be one reason for the high activity of $LaMnO_3$-based oxide.

Effects of dopant at the Mn site of $LaMnO_3$ were studied further. NO decomposition activities on the catalyst doped with Al and In, which are other elements in group 13 (or III B) of the periodic table, are also shown in Table 1. Although the activity of Al-doped $La_{0.7}Ba_{0.3}MnO_3$ catalyst in NO decomposition was slightly low, the catalyst doped with In exhibited the highest N_2 yield, which is comparable with that of the Ga-doped catalyst. The yield of O_2 was slightly higher over the catalyst doped with In than over that doped with Ga. Therefore, from a stability point of view, the In-doped catalyst is more promising than the Ga-doped catalyst. Consequently, in this study, NO decomposition on $LaMnO_3$ doped with Ba and In at the La and Mn sites, respectively, was investigated in detail.

In Table 1, the effects of alkaline earth cation at the La site on the activity of NO decomposition are also shown. Compared with the activity on the Sr- or Ca-doped catalyst, the Ba-doped catalyst exhibited much higher activity in NO direct decomposition. Consequently, barium is a better dopant at the La site of $LaMn_{0.8}In_{0.2}O_3$ for NO decomposition. In the following section, the content of dopant will be optimized.

3.2. Effects of Ba and In contents on NO decomposition activity of $LaMnO_3$ catalyst

Fig. 1 shows the XRD patterns of the $La_{0.7}Ba_{0.3}Mn_{1-x}In_xO_3$ catalyst. It is clear that strong main diffraction peaks could be assigned to those from $LaMnO_3$, and weak diffraction peaks from a secondary phase close to the main peaks, which may be In_2O_3, were also observed when the amount of In was higher than 20 mol%. Therefore, it can be said that the main phase of the sample is $LaMnO_3$. However, the limit of the solid solution of In at the Mn site of $LaMnO_3$ seems to exist between $x = 0.1$ and 0.2 in $La_{0.7}Ba_{0.3}Mn_{1-x}In_xO_3$ and a small amount of In_2O_3 is formed. The amount of In_2O_3 is negligibly small, because the diffraction peak from In_2O_3 is weak. On the other hand, diffraction peaks from $LaMnO_3$ are shifted to a lower angle with increasing amounts of In. Because the ionic sizes of In^{3+} and Mn^{3+} with the six coordination number are 640 and 500 pm, respectively, expansion of the lattice parameter with increasing In amount suggests that added In replaced the lattice position of Mn in the $LaMnO_3$ perovskite lattice.

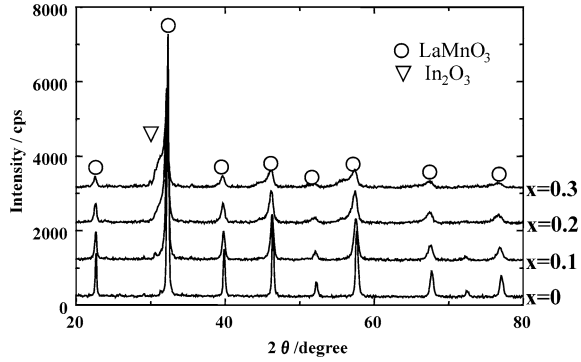

Fig. 1. XRD patterns of the $La_{0.7}Ba_{0.3}Mn_{1-x}In_xO_3$ catalyst.

Fig. 2 shows the conversion of NO into N_2, N_2O, and O_2 on $La_{0.7}Ba_{0.3}In_xMn_{1-x}O_3$ at 1073 K as a function of the value of x. Similar to the results reported by Teraoka et al. [10], the activity of $La_{0.7}Ba_{0.3}MnO_3$ in NO decomposition was low in this study. The yield of N_2 and O_2 increase with increasing In amounts and attain the maximum at $x = 0.2$. Therefore, the optimum amount for In doping seems to exist around $x = 0.2$. Since the amount of O_2 formation greatly increases with In doping, improved NO decomposition activity is considered to result from weakening O_2 adsorption on the catalyst. Here it is also obvious that the BET surface area is almost the same on all catalysts, and so

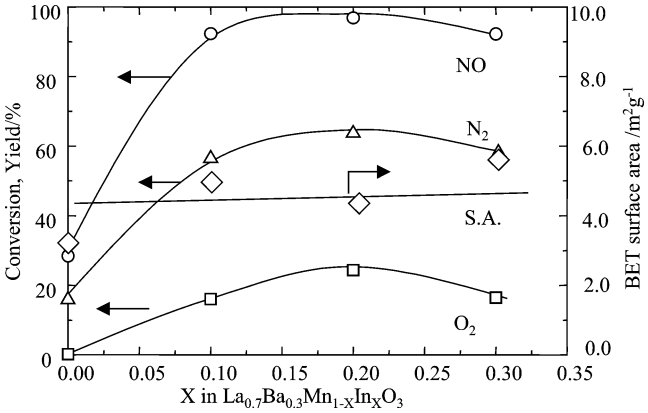

Fig. 2. Conversion of NO and yield of N_2 and O_2 on $La_{0.7}Ba_{0.3}In_x Mn_{1-x}O_3$ at 1073 K as a function of x (NO: 1%; He: balance; $W/F = 3\ g_{cat}\ s\ cm^{-3}$).

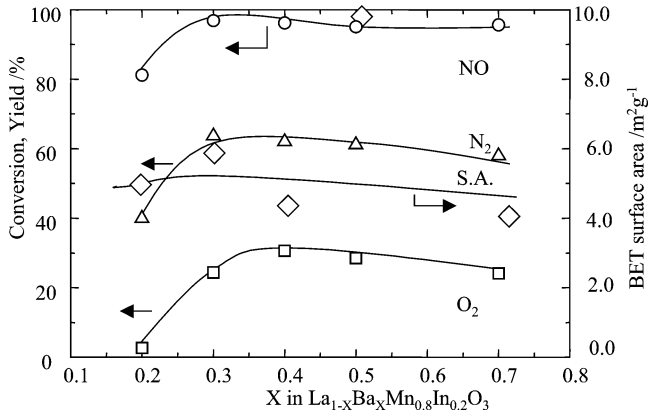

Fig. 4. NO conversion and yield of N_2 and O_2 at 1073 K as a function of x in $La_{1-x}Ba_xMn_{0.8}In_{0.2}O_3$ (NO: 1%; He: balance; $W/F = 3\ g_{cat}\ s\ cm^{-3}$).

increased NO decomposition activity cannot be explained by the geometrical effects. Because excessively added In results in the formation of In_2O_3, as detected by XRD, the activity of In_2O_3 in NO decomposition was also investigated. The results are shown in Table 1, where it is seen that the activity of In_2O_3 oxide in NO decomposition is low. Therefore, the influence of the impurity phase of In_2O_3 seems to be negligible in NO decomposition and the improved NO decomposition activity can be assigned to the chemical effects of In doped into the $LaMnO_3$ lattice.

The effects of Ba amount at the La site on NO decomposition activity were further studied, and XRD patterns of $La_{1-x}Ba_xMn_{0.8}In_{0.2}O_3$ are shown in Fig. 3. XRD patterns of the obtained $La_{1-x}Ba_xMn_{0.7}In_{0.3}O_3$ specimens also consist of diffraction peaks from $LaMnO_3$ and In_2O_3 in the range of $x = 0.2$–0.4 in $La_{1-x}Ba_xMn_{0.8}In_{0.2}O_3$. On the other hand, the diffraction peak from the $BaMnO_3$ phase appears at $x = 0.5$ and becomes the main peak at $x = 0.7$. Therefore, $LaMnO_3$ perovskite is still the main phase at low Ba content; however, $BaMnO_3$ is the main phase when x in $La_{1-x}Ba_xMn_{0.8}In_{0.2}O_3$ is higher than 0.5.

Fig. 4 shows the NO conversion and the yield of N_2, N_2O, and O_2 at 1073 K as a function of x in $La_{1-x}Ba_xMn_{0.8}In_{0.2}O_3$. It is clear that NO conversion as well as N_2 yield increase with increasing x and attain the maximum at $x = 0.3$. Therefore, the optimum amount of Ba addition seems to exist at $x = 0.3$. From the above results, it can be concluded that the highest activity of NO decomposition on Ba- and In-doped $LaMnO_3$ is attained at $La_{0.7}Ba_{0.3}Mn_{0.8}In_{0.2}O_3$ among the $LaMnO_3$ perovskite oxides.

The temperature dependence of NO conversion into N_2 and O_2 on $La_{0.7}Ba_{0.3}Mn_{0.8}In_{0.2}O_3$ is shown in Fig. 5. Obviously, NO decomposition proceeds from 873 K, and O_2 formation is also observed at temperatures higher than 973 K. The amount of O_2 formed is always smaller than that of N_2. However, if the formation of NO_2 is considered, the amounts of nitrogen and oxygen are almost balanced with the amount of NO converted. Therefore, it seems likely that no accumulation of oxygen on the catalyst occurred. In the following, NO decomposition activity is discussed mainly with the yield of N_2.

Fig. 6 shows the conversion of NO and the yield of N_2, N_2O, and O_2 at 1073 K as a function of time on stream. It is obvious that the conversion of N_2 attains a

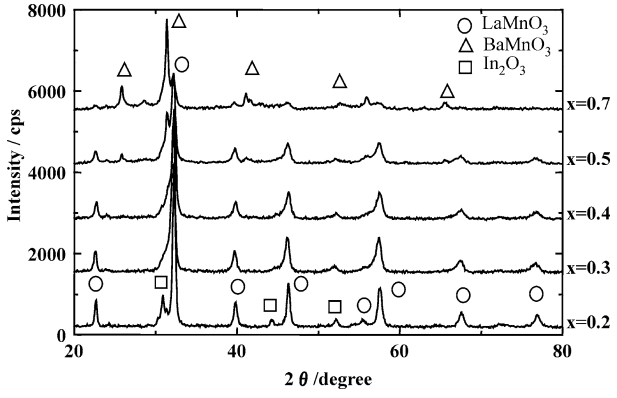

Fig. 3. XRD patterns of $La_{1-x}Ba_xMn_{0.8}In_{0.2}O_3$ catalyst.

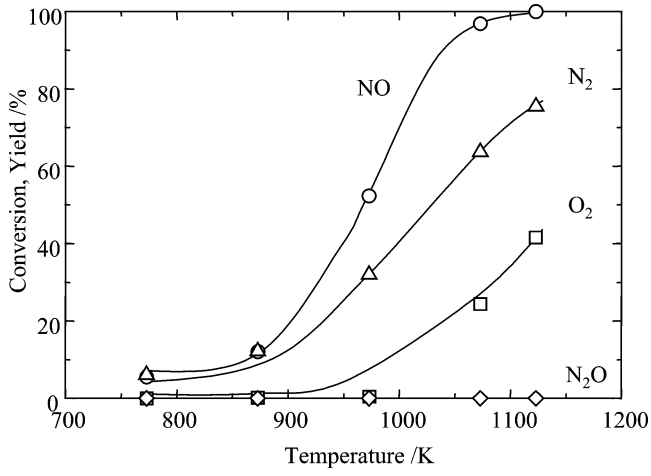

Fig. 5. Temperature dependence of NO conversion and yield of N_2 and O_2 on $La_{0.7}Ba_{0.3}Mn_{0.8}In_{0.2}O_3$ (NO: 1%; He: balance; $W/F = 3\ g_{cat}\ s\ cm^{-3}$).

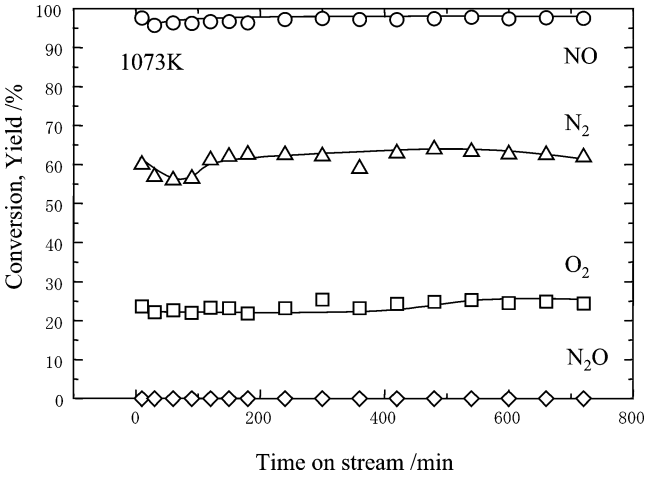

Fig. 6. Conversion of NO and yield of N_2 and O_2 at 1073 K on $La_{0.7}Ba_{0.3}Mn_{0.8}In_{0.2}O_3$ as a function of time on stream (NO: 1%; He: balance; $W/F = 3\ g_{cat}\,s\,cm^{-3}$).

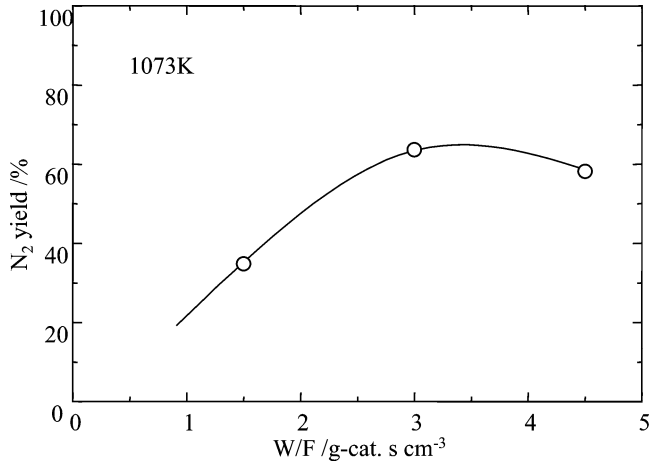

Fig. 7. Effects of contact time on N_2 yield on $La_{0.7}Ba_{0.3}Mn_{0.8}In_{0.2}O_3$ at 1073 K (NO: 1%; He: balance).

value of 64% at 1073 K during the initial 15 min and it is quite stable over 12 h. Therefore, perovskite oxide of $La_{0.7}Ba_{0.3}Mn_{0.8}In_{0.2}O_3$ exhibits a stable activity in NO direct decomposition, and considering the time dependence of N_2 formation, the high activity of NO decomposition will be exhibited for longer periods. In any case, it is obvious that $La_{0.7}Ba_{0.3}Mn_{0.8}In_{0.2}O_3$ exhibits stable activity in NO decomposition. In the previous study, it was generally considered that the catalytic activity of $LaMnO_3$-based oxide in NO decomposition was low; however, this study reveals that In-doped $LaMnO_3$ is active in NO direct decomposition, which is comparable with that of $LaCoO_3$-based oxide as a well-known active NO direct decomposition catalyst [14]. The improvement in NO decomposition activity could be assigned to weakening of the oxygen adsorption; this will be discussed later.

3.3. Effects of reaction condition on NO direct decomposition activity

Fig. 7 shows the effects of contact time on NO decomposition activity. It is seen that N_2 yield gradually decreases with decreasing contact time and at $W/F = 1.5\ g_{cat}\,h/mol$, N_2 yield is 35%. Although lower conversion in shorter contact time is generally observed in all heterogeneous catalytic reactions, the decrease in NO decomposition activity on this catalyst is slightly significant as the contact time decreases. This decrease in N_2 yield with decreasing contact time might be attributed to the low BET surface area, since the BET surface area of $La_{0.7}Ba_{0.3}Mn_{0.8}In_{0.2}O_3$ is as low as 8.0 m^2/g. For removal of NO_x in exhaust gas from an internal combustion engine, high activity at much shorter contact time is required. Therefore, increasing the BET surface area may be the most effective method for improving the NO decomposition activity on $La_{0.7}Ba_{0.3}Mn_{0.8}In_{0.2}O_3$ catalyst at shorter contact times. This is now under investigation and the results will be reported in the future.

The effects of coexisting oxygen on the N_2 formation rate were further studied, and results are shown in Fig. 8. Oxygen strongly adsorbs on the catalyst and decreases the NO decomposition activity. Therefore, only a limited number of catalysts show stable NO decomposition activity under the coexistence of oxygen. Teraoka et al. reported that $Sr_{0.6}La_{0.4}Mn_{0.8}Ni_{0.2}O_3$ can decompose NO into N_2 under coexistence of O_2 up to 10% [10]. As shown in Fig. 8, analogous to the results with $SrMnO_3$-based oxide, N_2 yield monotonically decreases with increasing O_2 concentration. Therefore, it seems likely that the coexisting oxygen strongly adsorbs on the active site of $La_{0.7}Ba_{0.3}Mn_{0.8}In_{0.2}O_3$ and, consequently, the coexisting oxygen strongly interferes with the NO decomposition reaction. However, even under 10% O_2 coexistence, $La_{0.7}Ba_{0.3}Mn_{0.8}In_{0.2}O_3$ catalyst can proceed in the NO decomposition reaction and the N_2 yield is sustained at 12%.

To analyze the reaction mechanism kinetically, P_{O_2} and P_{NO} dependences on N_2 formation rate were estimated.

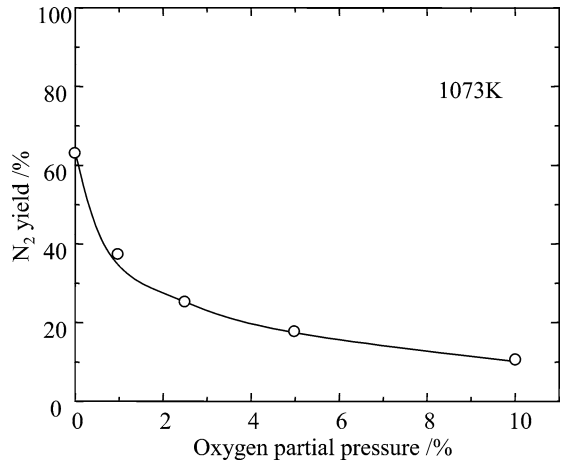

Fig. 8. Effects of coexisting oxygen on N_2 formation rate on $La_{0.7}Ba_{0.3}Mn_{0.8}In_{0.2}O_3$ at 1073 K (NO: 1%; He: balance; $W/F = 3\ g_{cat}\,s\,cm^{-3}$).

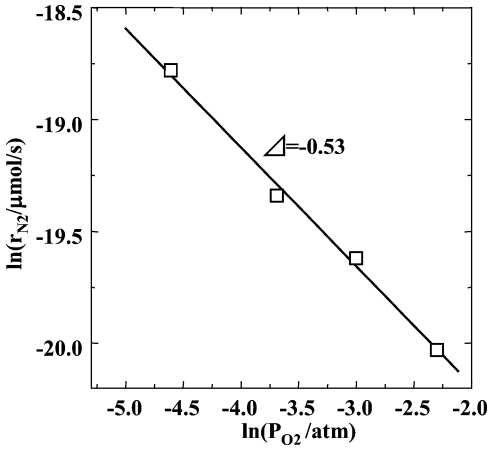

Fig. 9. N_2 formation rate on $La_{0.7}Ba_{0.3}Mn_{0.8}In_{0.2}O_3$ as a function of oxygen partial pressure at 1073 K.

Fig. 9 shows the N_2 formation rate as a function of oxygen partial pressure. It is obvious that the N_2 formation rate monotonically decreases with increasing oxygen partial pressure and the P_{O_2} dependence is estimated to be -0.53, which is similar to the value reported for $SrMnO_3$-based oxide. Fig. 10 shows the N_2 formation rate as a function of NO partial pressure. In contrast to the effects of coexisting oxygen, N_2 formation rate monotonically increases with increasing NO partial pressure. The dependence of N_2 formation rate on NO partial pressure is estimated to be 1.31. Therefore, the rate-determining step for NO decomposition on $La_{0.7}Ba_{0.3}Mn_{0.8}In_{0.2}O_3$ seems to be related to the adsorption or activation of NO. The N_2 formation rate for NO decomposition as a function of O_2 and NO partial pressures has already been reported by Teraoka et al. for $La_{0.4}Sr_{0.6}Mn_{0.8}Ni_{0.2}O_3$, and P_{NO} and P_{O_2} dependences on this catalyst are 1.04 and -0.16, respectively [10]. Therefore, the estimated reaction order of N_2 formation rate for NO and O_2 partial pressure on $La_{0.7}Ba_{0.3}Mn_{0.8}In_{0.2}O_3$ can be almost the same as that reported for $La_{0.4}Sr_{0.6}Mn_{0.8}Ni_{0.2}O_3$ [10]. On the other hand,

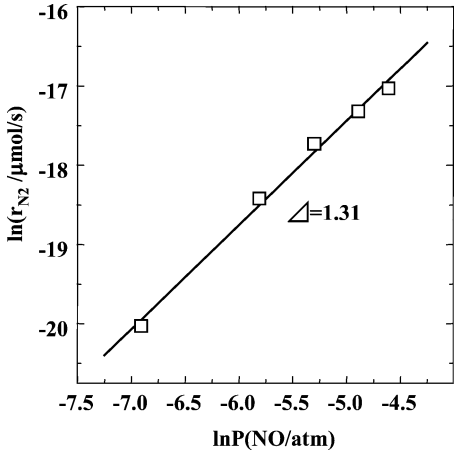

Fig. 10. N_2 formation rate on $La_{0.7}Ba_{0.3}Mn_{0.8}In_{0.2}O_3$ as a function of NO partial pressure at 1073 K.

it is also noted that fairly close values for NO and O_2 dependence have been reported for La_2O_3 [15] and Ba/MgO [8].

3.4. Adsorption states of NO and O_2 by DRIFTS

To study the effects of In at the Mn site of the $LaMnO_3$ catalyst on the adsorption states of NO and O_2, the adsorption states of NO and O_2 on $La_{0.7}Ba_{0.3}Mn_{0.8}In_{0.2}O_3$ and $La_{0.7}Ba_{0.3}MnO_3$ were measured with diffuse reflectance FT-IR spectroscopy (DRIFTS). The number of reports on the NO adsorption state of Mn-based oxide has been rather limited so far, and the adsorption state on Mn-based oxide has not been studied sufficiently [16]. Fig. 11 shows DRIFTS spectra of absorbed NO at various temperatures for 1 h. After introduction of NO at 873 K, absorption peaks appear at 2343 and 2333 cm^{-1}, which could be assigned to N_2O species. With increasing temperature, a broad absorption band appears around 1100 and a sharp absorption band at 1349 cm^{-1}. This could be assigned to nitrate (NO_3^-) or nitrite (NO_2^-) species according to the assignment of Vannice and co-workers on La_2O_3 oxide [15]. Because the difference in the IR spectra of NO_2^- and NO_3^- is not large, adsorption species at 1363 cm^{-1} could not be easily assigned only with this experiment. However, considering that adsorption bands appeared at 1180, 1114, and 1076 cm^{-1}, it seems most likely that the adsorption species at 1363 cm^{-1} could be assigned to the unidentate nitrate ($MONO_2$, where M is metal). In addition, unidentate and bidentate NO_3^- are easily formed on MnO_2 [16]. Although further detailed study is required, we tentatively assign this ionic derivative from NO as NO_3^- in this study.

Adsorption bands also appeared at 1629 and 1513 cm^{-1}, which could be assigned to bent-type NO adsorption (NO^-) considering the adsorption frequency [15]. After evacuation at room temperature, the absorption band at 1629 cm^{-1} disappeared. Therefore, two absorption peaks could be assigned to the NO^- species adsorbed at the different adsorption sites.

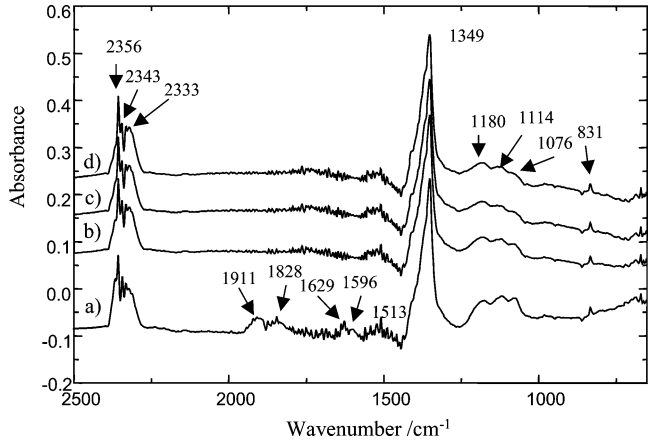

Fig. 11. DRIFTS spectra of NO absorbed on $La_{0.7}Ba_{0.3}Mn_{0.8}In_{0.2}O_3$ at various temperatures for 1 h. (a) NO adsorption at 873 K in NO (13.32 kPa); (b) evacuation at 298 K for 1 h; (c) evacuation at 473 K for 1 h; (d) evacuation at 673 K for 1 h.

It is considered that the NO^- adsorption species appearing at 1629 cm^{-1} is weak and this nitrosyl species easily desorbed at low temperature. On the other hand, absorbance of the peak at 1513 cm^{-1}slightly decreased after evacuation at 673 K. Therefore, another bent-type NO seems to be a rather stable adsorption species. In contrast, the intensity of absorption bands at 1349, 1180, 1114, 1076, and 831 cm^{-1} hardly changed after evacuation at 673 K for 1 h. Therefore, adsorption of NO_3^- is strong and covers the catalyst surface. Considering the change in the IR spectra of NO, the activation of NO proceeds through the bent-type adsorption and, at the first step, NO^- species couple to form N_2O and surface oxygen ($2NO = N_2O + O_{ad}$). Surface N_2O further decomposes to form N_2 and surface oxygen. In the following steps, gaseous NO or adsorbed NO reacts with surface oxygen to form NO_3^- or NO_2^- species. Here the charge neutrality for the formation of NO_3^- or NO_2^- species can be retained by oxidation of Mn^{3+} cation to form Mn^{4+}. The formation of N_2 is also observed by mass spectroscopy in the gas phase. Thus, formed NO_3^- is the strong adsorption species and covers the active site on the $La_{0.7}Ba_{0.3}MnO_3$ catalyst. Because formation of N_2O was not detected in the reaction by gas chromatograph analysis, N_2O seems to be the adsorption species on the catalysts and decomposition of N_2O is too fast to observe in the gas phase. However, IR measurement clearly suggests that NO direct decomposition seems to proceed via N_2O as the intermediate reaction species. N_2O is considered to be an intermediate in the NO selective reduction of NH_3 and direct decomposition on La_2O_3 [15] and Ba/MgO [7].

3.5. Adsorption states of NO and O_2 by TPD and reaction mechanism

Effects of In on NO and O_2 adsorption states were studied with temperature-programmed desorption (TPD) techniques. Fig. 12 shows desorption profiles of oxygen from $La_{0.7}Ba_{0.3}Mn_{0.8}In_{0.2}O_3$ and $La_{0.7}Ba_{0.3}MnO_3$ oxide. It can be seen that desorption of oxygen occurs only at temperatures higher than 773 K on both catalysts. Therefore, adsorption of oxygen on these catalysts is strong. On the other hand, the amount of desorbed oxygen greatly increases with In doping at the Mn site of $La_{0.7}Ba_{0.3}MnO_3$. Because no O_2 desorption was observed on In_2O_3 oxide up to 1073 K, the increased amount of oxygen is not caused by the decomposition of In_2O_3. Therefore, it is obvious that In doping is effective for decreasing the adsorption strength of oxygen, resulting in improved activity in NO decomposition. Fig. 13 show the NO desorption profiles from $La_{0.7}Ba_{0.3}Mn_{0.8}In_{0.2}O_3$ and $La_{0.7}Ba_{0.3}MnO_3$ oxides. In this figure, desorption of N_2 and O_2, which forms from the adsorbed NO, is also shown. Desorption of NO occurs in three different temperature ranges, namely, two peaks at low (around 373 K and around 473 K) and one at high (around 873 K) temperature, from both catalysts. The desorption of O_2 is observed in a high temperature range on both catalysts. However, desorption of N_2 is not observed at high temperature on $La_{0.7}Ba_{0.3}MnO_3$, while a small amount of N_2 formation is observed on $La_{0.7}Ba_{0.3}Mn_{0.8}In_{0.2}O_3$. On the other hand, a small amount of N_2 desorption is observed on both catalysts at low temperatures (373–573 K). The amount of N_2 desorption is much smaller than that of O_2. N_2 formation is also observed during NO adsorption at 773 K. Although the amount of N_2 formed was not quantitatively analyzed

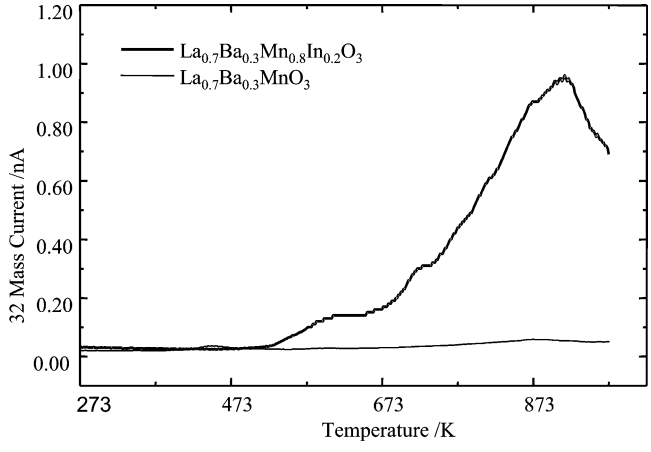

Fig. 12. O_2-TPD profiles ($m/e = 32$) from $La_{0.7}Ba_{0.3}Mn_{0.8}In_{0.2}O_3$ and $La_{0.7}Ba_{0.3}MnO_3$ oxide.

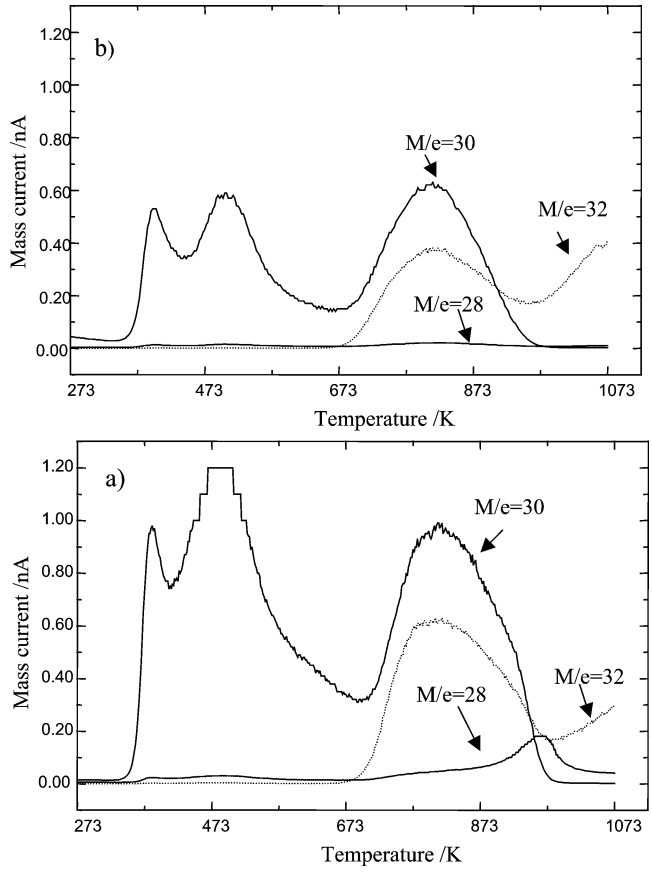

Fig. 13. NO-TPD profiles ($m/e = 30$) from $La_{0.7}Ba_{0.3}Mn_{0.8}In_{0.2}O_3$ (a) and $La_{0.7}Ba_{0.3}MnO_3$ (b) oxides.

in this study, the disproportionation reaction ($3NO + e = N_2 + NO_3^-$) may occur during adsorption at 773 K, resulting in the formation of NO_3^- species on the surface. Here, e is formed by the oxidation of Mn^{3+} in the catalyst; i.e., $Mn^{3+} = Mn^{4+} + e$. Considering that Mn^{4+} is stable in a perovskite lattice, NO_3^- may also be related to the oxidation of Mn^{3+} to Mn^{4+}.

On the other hand, a fairly large amount of O_2 desorption was observed at temperatures higher than 673 K. Because it is well known that the lattice oxygen also desorbs in the same temperature range as $LaMnO_3$-based oxide [17], the origin of desorbed oxygen was studied with $^{18}O_2$ adsorption. Fig. 14 shows the oxygen desorption profiles of $La_{0.7}Ba_{0.3}Mn_{0.8}In_{0.2}O_3$ when $^{18}O_2$ is used for the adsorbent. $^{18}O\,^{18}O$ desorption is observed around 373 K and in the temperature range 673 to 873 K. In the same temperature range, $^{16}O\,^{17}O$ desorption also occurs. Therefore, desorption of oxygen around 873 K can be assigned to the adsorbed oxygen or surface weakly bonded oxygen. It is also considered that a large part of oxygen adsorbing on $La_{0.7}Ba_{0.3}Mn_{0.8}In_{0.2}O_3$ catalyst is dissociative, and recombination between the adsorbed and the lattice oxygen easily occurs during desorption. However, desorption of $^{18}O\,^{16}O$ as well as $^{18}O\,^{18}O$ is almost negligible, while that of $^{16}O\,^{16}O$ is still large at temperatures higher than 973 K. Therefore, oxygen desorption above 973 K could be assigned to the lattice oxygen which may be desorbed by reduction of Mn^{3+}.

Because the amount of O_2 desorbed is smaller in NO-TPD than that in O_2-TPD and the desorption of adsorbed oxygen is complete at 973 K, the O_2 desorbed during NO-TPD seems to form through decomposition of NO_3^- species into NO and O_2 ($NO_3^- = NO + O_2 + e$) and not through simple desorption of the lattice oxygen. Here, the formed electron is also consumed by the reduction of Mn^{4+} to Mn^{3+}, which is the opposite reaction for the formation of NO_3^-.

Considering the IR measurements, desorption of NO at three temperatures could be assigned to the molecularly adsorbed NO (may be weakly or strongly adsorbed NO^-) and

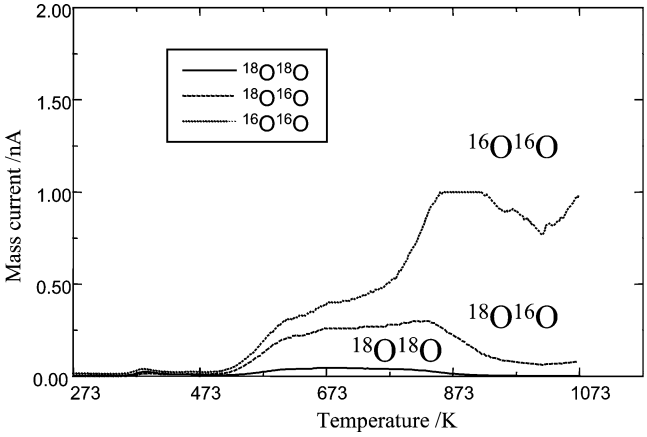

Fig. 14. O_2 isotopic TPD profile of $La_{0.7}Ba_{0.3}Mn_{0.8}In_{0.2}O_3$ after $^{18}O_2$ adsorbs at 873 K for 0.5 h.

NO_3^- species which formed by disproportionate adsorption of NO ($3NO + e = N_2 + NO_3^-$) or adsorption of NO on the strongly adsorbed surface oxygen ($NO + 2O^{2-} = NO_3^- + 3e$), which may be formed during the primary NO decomposition. In fact, N_2 but not O_2 formation was observed around 473 K in NO-TPD (Fig. 13). This may suggest that partial NO decomposition ($2NO + 4e = N_2 + 2O^{2-}$) occurs on this catalyst at decreased temperature. If gaseous NO adsorbs on the surface oxygen which is formed by partial NO decomposition, the overall reaction could be written as disproportionate adsorption of NO. This may be a more reasonable mechanism for the formation of NO_3^-. NO direct decomposition occurs at temperatures higher than 873 K, as shown in Fig. 9, and at the same temperature, desorption of NO and O_2 occurs. Therefore, it seems likely that NO decomposition occurs after removal of NO_3^- species from the surface, which is also related to the thermal reduction of Mn^{4+} to Mn^{3+}. On the other hand, the In-doped catalyst exhibits much larger NO desorption amounts in low and high temperature ranges. Therefore, NO adsorption is also improved by In doping, because the BET surface area of both catalysts is almost the same, as shown in Fig. 2. Doped In has positive effects in improving NO adsorption by serving the adsorption site, which might be an oxygen vacancy. In addition, In doping has also positive effects in weakening oxygen adsorption. Therefore, the NO decomposition activity of $La_{0.7}Ba_{0.3}MnO_3$ is greatly increased by In doping at the Mn site.

3.6. N_2O and NO_2 direct decomposition reaction as a model reaction

Although the formation of N_2O was not detected in the NO decomposition reaction on $La_{0.7}Ba_{0.3}Mn_{0.8}In_{0.2}O_3$, IR measurement suggests formation of N_2O after exposure to NO at temperatures lower than 673 K. To confirm the contribution of N_2O as an intermediate in direct NO decomposition, direct decomposition of N_2O on $La_{0.7}Ba_{0.3}Mn_{0.8}In_{0.2}O_3$ catalyst was also investigated in this study. The temperature dependence of N_2O decomposition activity on $La_{0.7}Ba_{0.3}Mn_{0.8}In_{0.2}O_3$ catalyst is shown in Fig. 15. It is seen that this $La_{0.7}Ba_{0.3}Mn_{0.8}In_{0.2}O_3$ catalyst is highly active for N_2O decomposition as expected and the complete decomposition of N_2O is achieved at temperatures as low as 773 K. In addition, the amount of N_2 and O_2 formed is similar to that of N_2O converted. Fig. 16 shows the effects of coexisting oxygen on N_2O decomposition activity. Although the activity of N_2O decomposition decreased, the temperature for complete decomposition increased with the concentration of oxygen. However, N_2O decomposition on $La_{0.7}Ba_{0.3}Mn_{0.8}In_{0.2}O_3$ still proceeded under the coexistence of 10% O_2, and 100% N_2O decomposition was achieved at 900 K. Consequently, if N_2O forms, the decomposition of N_2O occurs quickly on this catalyst, and in NO decomposition in the fixed bed reactor, formation of N_2O is not observed. However, N_2O is considered

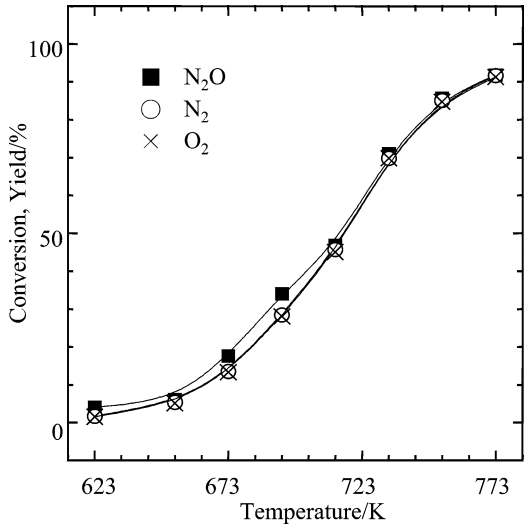

Fig. 15. Temperature dependence of N_2O decomposition activity on $La_{0.7}Ba_{0.3}Mn_{0.8}In_{0.2}O_3$ catalyst (N_2O: 10%; He: balance; $W/F = 3\ g_{cat}\ s\ cm^{-3}$).

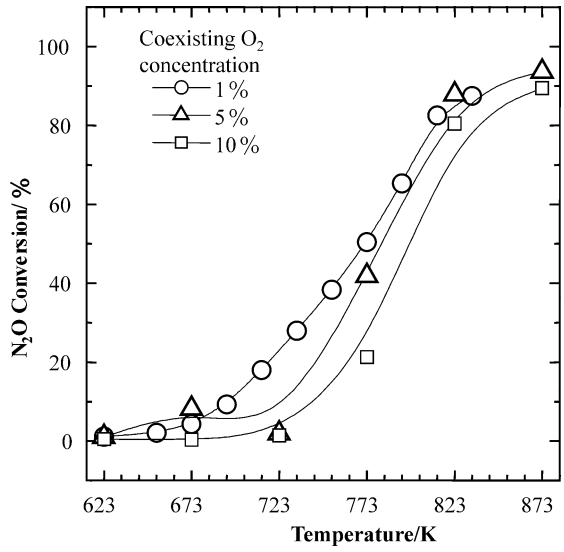

Fig. 16. Temperature dependence of N_2O decomposition activity on $La_{0.7}Ba_{0.3}Mn_{0.8}In_{0.2}O_3$ catalyst under coexistence of oxygen (N_2O: 10%; He: balance; $W/F = 3\ g_{cat}\ s\ cm^{-3}$).

the intermediate species because decomposition of N_2O is highly active on $La_{0.7}Ba_{0.3}Mn_{0.8}In_{0.2}O_3$. It is also noted that Mn_2O_3 is active in N_2O decomposition [18].

DRIFTS measurement suggests that NO_3^- species forms at elevated temperature. To evaluate the possibility of NO_3^- as an intermediate species, the NO_2 decomposition reaction was further investigated in this study. This is because NO_3^- species forms more easily from NO_2 than from NO. Fig. 17 shows the temperature dependence of yield of N_2 in NO_2 direct decomposition on $La_{0.7}Ba_{0.3}Mn_{0.8}In_{0.2}O_3$. In this figure N_2 yield in NO decomposition is also shown for comparison. It can be seen that NO_2 direct decomposition occurs on $La_{0.7}Ba_{0.3}Mn_{0.8}In_{0.2}O_3$ catalyst at temperatures higher than 873 K, and O_2 formation is also observed. However,

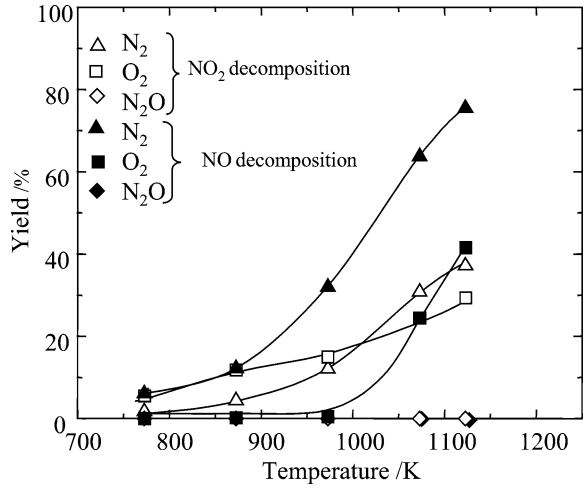

Fig. 17. Temperature dependence of yield of N_2 and O_2 in NO_2 and NO direct decomposition on $La_{0.7}Ba_{0.3}Mn_{0.8}In_{0.2}O_3$ (NO or NO_2: 1%; He: balance; $W/F = 3\ g_{cat}\ s\ cm^{-3}$).

N_2 yield is much smaller than that in NO direct decomposition. For the selective reduction of NO_x with hydrocarbon, the N_2 yield is higher for NO_2 than that for NO [1,19–21]. Therefore, selective reduction of NO is considered to occur through NO_2 or NO_2 derivatives. Some similarity in reaction mechanism is considered between the selective reduction and the direct reduction in the case of Cu-ZSM-5. However, in the case of $La_{0.7}Ba_{0.3}Mn_{0.8}In_{0.2}O_3$, it is apparent that the direct decomposition of NO on this catalyst does not proceed through NO_2 or NO_2 derivatives which may be NO_2^- or NO_3^-. Lunsford and co-workers also reported that ionic intermediates such as NO_3^- are highly stable and could account for the negative influence on NO direct decomposition on Ba/MgO catalyst with the coexistence of oxygen [8].

Because IR measurement suggests that the NO_3^- species is a strong adsorption species, removal of NO_3^- and/or surface oxygen from the active site seems to be the most important step in the NO decomposition reaction over this $LaMnO_3$-based perovskite oxide. Considering the strong adsorption of oxygen and NO_3^-, it is quite reasonable that the removal of oxygen or NO_3^- to form the vacant adsorption site is the important initial step in the NO direct decomposition reaction. Once a vacant adsorption site is formed, adsorption of NO smoothly occurs and NO decomposes into N_2 and O_2 through N_2O.

3.7. Reaction mechanism from kinetic analysis

The reaction steps expected from the DRIFTS and TPD data are as follows:

$$2NO + 2[s] = 2NO[s], \quad (1)$$

$$2NO[s] = N_2O[s] + O[s], \quad (2)$$

$$N_2O[s] = N_2 + O[s] \quad \text{(fast step)}, \quad (3)$$

$$2O[s] = O_2 + 2[s]. \quad (4)$$

Here [s] is the surface adsorption site. Because the activity observed for NO_2 decomposition was lower than that observed for NO, contribution of NO_2 in NO decomposition was not considered in this study. Since the desorption of NO occurs easily at low temperatures, it is reasonably expected that the adsorption of NO expressed by Eq. (1) is the rate-determining step in NO decomposition. The rate of decomposition of NO is expressed as follows, provided that the adsorption of NO [Eq. (1)] is the rate-limiting step:

$$r_{N_2} = \frac{(\vec{k_1} P_{NO}^2 - \overleftarrow{k_1} K_2 K_3 K_4^{-1} P_{N_2} P_{O_2})[S_0]^2}{(1 + \sqrt{K_2 K_3 K_4^{-1}} P_{N_2}^{1/2} P_{O_2}^{1/2} + K_4^{-1/2} P_{O_2}^{1/2})^2}. \quad (5)$$

Here, K_i represents the equilibrium constant of each equation i and $\vec{k_1}$ and $\overleftarrow{k_1}$ are the rate constants of the forward and reverse side reactions of NO adsorption [Eq. (1)], respectively. $[S_0]$ represents the total number of adsorption sites. In this equation, the concentration of the surface N_2O is assumed to be 0, since reactions (2) and (3) occur quickly. Because the partial pressure of N_2 is negligible, P_{N_2} can also be ignored under the experimental conditions. Therefore, Eq. (5) can be simplified as

$$r_{N_2} = \frac{(\vec{k_1} P_{NO}^2)[S_0]^2}{(1 + K_4^{-1/2} P_{O_2}^{1/2})^2}. \quad (6)$$

According to this equation, dependence of NO and O_2 partial pressure is given a value of 2 and a value between 0 and -1, respectively.

If the surface reaction step of Eq. (2) is the rate-limiting step, as suggested by Teraoka et al. [10] and Huang et al. [15], then the rate equation can be expressed as

$$r_{N_2} = \left(\vec{k_2} P_{NO}^2 - \overleftarrow{k_2} K_3^{-1} K_4^{-1} P_{N_2} P_{O_2}\right)[S_0]^2 \Big/ \left(1 + K_1^{1/2} P_{NO} + K_4^{-1/2} P_{O_2}^{1/2} + K_3^{-1} K_4^{-1/2} P_{N_2} P_{O_2}^{1/2}\right)^2. \quad (7)$$

Again, this equation can be simplified by assuming a small surface concentration of N_2O and small partial pressure of N_2 in the gas phase:

$$r_{N_2} = \frac{(\vec{k_2} P_{NO}^2)[\overleftarrow{S_0}]^2}{(1 + K_1^{1/2} P_{NO} + K_4^{-1/2} P_{O_2}^{1/2})^2}. \quad (8)$$

According to this equation, dependence of NO and O_2 partial pressure is given a value between 0 and 2 and between 0 and -1, respectively.

On the other hand, if the desorption of O_2 [Eq. (4)] is the rate-limiting step, which is also another reasonable rate-limiting step considering the results of TPD, the decomposition rate is expressed as

$$r_{N_2} = \frac{(\vec{k_4} K_1^{-1} K_2^{-1} K_3 P_{N_2}^{-1} P_{NO}^2 - \overleftarrow{k_4} P_{O_2})[S_0]^2}{(1 + K_1^{-1/2} P_{NO} + \sqrt{K_1 K_2 K_3} P_{N_2}^{-1/2} P_{NO})^2}. \quad (9)$$

Assuming that the partial pressure of N_2 is negligible, the rate of N_2 formation depends on the P_{NO} power of a value between 0 and -2 and P_{O_2} between 0 and -1.

The observed P_{NO} and P_{O_2} dependences of N_2 formation rate on $La_{0.7}Ba_{0.3}Mn_{0.8}In_{0.2}O_3$ catalyst are 1.3 and -0.5, respectively. Therefore, the rate equations (6) and (8) are almost consistent with the results observed in this study, suggesting that the adsorption of NO on the active site and/or the formation of N_2O is the rate-determining step. At present, we cannot determine from the present data which step is rate-determining. However, considering the strong adsorption of oxygen and/or NO_3^- species and the weak adsorption of molecular NO, the adsorption of NO seems most likely to be the rate-determining step on this catalyst. Because of the weakening adsorption of oxygen and/or NO_3^-, In doping at the Mn site is effective for increasing NO decomposition activity. Doped In does not form an oxygen vacancy because the valence number of In (+3) is the same as that of Mn (+3). Therefore, weakening of oxygen and/or NO_3^- adsorption species may originate from the improved mobility of oxygen vacancy in bulk.

4. Conclusion

In conventional study, a limited number of catalysts can proceed in NO direct decomposition. However, this study, we focused on improving oxygen mobility in bulk by doping various cations, and we found that In doping is highly effective for increasing NO direct decomposition activity of an La(Ba)MnO_3 catalyst. In spite of the negligible activity of In-based oxide in NO decomposition, the fact that NO direct decomposition of $LaMnO_3$ improved greatly with In doping is highly interesting from the viewpoint of developing new catalysts for NO decomposition. This study also revealed that $La_{0.7}Ba_{0.3}Mn_{0.8}In_{0.2}O_3$ is active in N_2O decomposition. At present, removal of N_2O is another important subject from an environmental perspective because N_2O is one of the greenhouse gases and mainly exhausted in the medical field [18,22]. The developed $La_{0.7}Ba_{0.3}Mn_{0.8}In_{0.2}O_3$ catalyst is expected to be applicable for N_2O removal.

The rate-limiting step for NO decomposition on this catalyst may be the adsorption of NO at the vacant site. Since the adsorption site is occupied by oxygen and/or NO_3^- species up to high temperatures, removal of oxygen from the surface is important. Because the doped In is highly effective at improving the mobility of oxygen vacancy in bulk, In doping In at the Mn site of $LaMnO_3$ is considered effective in increasing NO decomposition activity.

Acknowledgment

Part of this study was financially supported by a Grant-in-Aid for Science Promotion from the Ministry of Education, Culture, Sports, Science, and Technology of Japan (No. 11102006).

References

[1] M. Iwamoto, Shokubai 37 (1995) 614.
[2] S. Kagawa, Y. Teraoka, Hyomen 31 (1993) 913.
[3] H. Hamada, Shokubai 33 (1991) 320.
[4] M. Iwamoto, H. Yahiro, S. Shundo, Y. Yu-u, N. Mizuno, Appl. Catal. 69 (1991) L15.
[5] M. Iwamoto, H. Yahiro, K. Tanda, N. Mizuno, Y. Mine, S. Kagawa, J. Phys. Chem. 95 (1991) 3727.
[6] Y.F. Chang, J.G. McCarty, J. Catal. 178 (1998) 408.
[7] M.A. Vannice, A.B. Walters, X.J. Zhang, J. Catal. 159 (1996) 119.
[8] S. Xie, M.P. Rosynek, J.H. Lunsford, J. Catal. 188 (1999) 24.
[9] Y. Teraoka, H. Fukuda, S. Kagawa, Chem. Lett. (1990) 1.
[10] Y. Teraoka, T. Harada, S. Kagawa, J. Chem. Soc., Faraday Trans. 94 (1998) 1887.
[11] D. Klvana, J. Kirchnerova, C. Tofan, Korean J. Chem. Eng. 16 (1999) 470.
[12] T. Ishihara, H. Matsuda, Y. Takita, J. Am. Chem. Soc. 16 (1994) 3801.
[13] T. Mori, H. Yamamura, H. Ogino, H. Kobayashi, T. Mitamura, J. Am. Ceram. Soc. 77 (1994) 2771.
[14] K. Tabata, M. Misono, Catal. Today 8 (1990) 175.
[15] S.J. Huang, A.B. Walters, M.A. Vannice, J. Catal. 192 (2000) 29.
[16] M. Mchida, M. Uto, D. Kurogi, T. Kijima, J. Mater. Chem. 11 (2001) 900.
[17] H.M. Zhang, N. Yamazoe, Y. Teraoka, J. Mater. Sci. Lett. 8 (1989) 995.
[18] T. Yamashita, A. Vannice, J. Catal. 161 (1996) 254.
[19] D.B. Lukyanov, G. Sill, J.L. d'Itri, W.K. Hall, J. Catal. 153 (1995) 265.
[20] T. Ishihara, M. Kagawa, F. Hadama, Y. Takita, J. Catal. 169 (1997) 93.
[21] Y. Li, N. Armor, J. Catal. 150 (1994) 376.
[22] Y. Yuzaki, T. Tarimizu, S. Ito, K. Kunimori, Catal. Lett. 47 (1997) 173.